Inorganic Chemistry
including bioinorganic chemistry

Subscriber access provided by OAK RIDGE NATIONAL LAB

Article

Magnetic Compensation and Ordering in the Bimetallic Oxalates: Why Are the 2D and 3D Series so Different?

Randy S. Fishman, Miguel Clemente-Leo#n, and Eugenio Coronado

Inorg. Chem., **2009**, 48 (7), 3039-3046• Publication Date (Web): 02 March 2009

Downloaded from http://pubs.acs.org on March 30, 2009

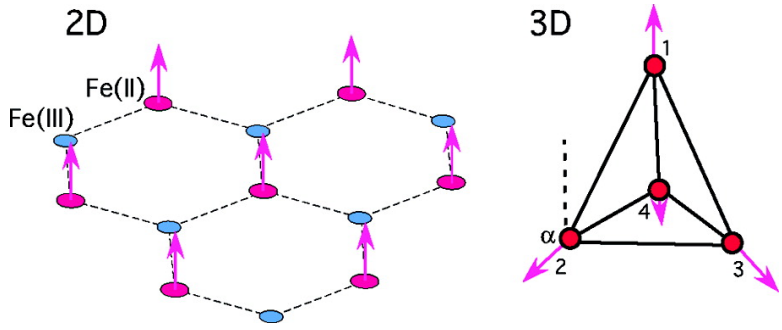

More About This Article

Additional resources and features associated with this article are available within the HTML version:

- Supporting Information
- Access to high resolution figures
- Links to articles and content related to this article
- Copyright permission to reproduce figures and/or text from this article

View the Full Text HTML

ACS Publications
High quality. High impact.

Inorganic Chemistry is published by the American Chemical Society. 1155 Sixteenth Street N.W., Washington, DC 20036

Inorg. Chem. **2009**, *48*, 3039−3046

Magnetic Compensation and Ordering in the Bimetallic Oxalates: Why Are the 2D and 3D Series so Different?

Randy S. Fishman,*,† Miguel Clemente-León,‡,§ and Eugenio Coronado‡

Materials Science and Technology Division, Oak Ridge National Laboratory, Oak Ridge, Tennessee 37831-6071, Instituto de Ciencia Molecular, Universidad de Valencia, Polígono de la Coma s/n, 46980 Paterna, Spain, and Fundació General de la Universitat de València (FGUV)

Received December 8, 2008

Although the exchange coupling and local crystal-field environment are almost identical in the two-dimensional (2D) and three-dimensional (3D) series of bimetallic oxalates, those two classes of materials exhibit quite different magnetic properties. Using mean-field theory to treat the exchange interaction, we evaluate the transition temperatures and magnetizations of the 3D Fe(II)Fe(III) and Mn(II)Cr(III) bimetallic oxalates. Because of the tetrahedral coordination of the chiral anisotropy axis, the 3D bimetallic oxalates have lower transition temperatures than their 2D counterparts, and much stronger anisotropy is required to produce magnetic compensation in the 3D Fe(II)Fe(III) compounds. The spin−orbit coupling with the non-collinear orbital moments causes the spins to cant in both 3D compounds.

I. Introduction

One of the most exciting developments in coordination chemistry has been the ability to control the dimension of materials with essentially the same molecular building blocks. Two-dimensional (2D) and three-dimensional (3D) bimetallic oxalates[1] are constructed from the same building block: an oxalate molecule ox = $C_2O_4^{2-}$ bridging transition-metal ions M(II) and M′(III). This extensive family of compounds exhibits unusual magnetic behavior ranging from magnetic compensation[2] to magneto-chiral dichroism.[3] Their hybrid structure permits the design of multifunctional materials in which the magnetism of the oxalate network coexists with the electronic properties of the cationic molecular lattice. For example, paramagnetic decamethylferrocenium[4] or spin-crossover cations,[5] photochromic[6] or NLO-active molecules,[7] organic π-electron donors,[8] and chiral cations[3,9−11] produce magnetic multilayers, photochromic magnets, ferromagnetic molecular metals, and chiral magnets, respectively.

Despite their different dimensionality, the 2D and 3D bimetallic oxalates would seem quite similar. Transition-metal ions in both series of compounds have three nearest

* To whom correspondence should be addressed. E-mail: fishmanrs@ornl.gov.
† Oak Ridge National Laboratory.
‡ Instituto de Ciencia Molecular, Universidad de Valencia.
§ Fundació General de la Universitat de València.

(1) See the reviews: (a) Clément, R.; Decurtins, S.; Gruselle, M.; Train, C. *Monatsh. Chem.* **2003**, *134*, 117. (b) Gruselle, M.; Train, C.; Boubekeur, K.; Gredin, P.; Ovanesyan, N. *Coord. Chem. Rev.* **2006**, *250*, 2491.
(2) (a) Mathonière, C.; Carling, S. G.; Day, P. *J. Chem. Soc., Chem. Commun.* **1994**, 1551. (b) Mathonière, C.; Nuttall, C. J.; Carling, S. G.; Day, P. *Inorg. Chem.* **1996**, *35*, 1201. (c) Nutall, C. J.; Day, P. *Chem. Mater.* **1998**, *10*, 3050.
(3) Train, C.; Gheorghei, R.; Krstic, V.; Chamoreau, L. M.; Ovanesyan, N. S.; Rikken, G. L. J. A.; Gruselle, M.; Verdaguer, M. *Nat. Mater.* **2008**, *17*, 729.
(4) (a) Clemente-León, M.; Galán-Mascarós, J. R.; Gómez-García, C. J. *Chem. Commun.* **1997**, 1727. (b) Coronado, E.; Galán-Mascarós, J. R.; Gómez-García, C. J.; Martínez-Agudo, J. M. *Adv. Mater.* **1999**, *11*, 558. (c) Coronado, E.; Galán-Mascarós, J. R.; Gómez-García, C. J.; Ensling, J.; Gutlich, P. *Chem.—Eur. J.* **2000**, *6*, 552.
(5) Clemente-León, M.; Coronado, E.; Giménez-López, M. C.; Soriano-Portillo, A.; Waerenborgh, J. C.; Delgado, F. S.; Ruiz-Perez, C. *Inorg. Chem.* **2008**, *47*, 9111.
(6) (a) Bénard, S.; Yu, P.; Audière, J. P.; Rivière, E.; Clément, R.; Ghilhem, J.; Tchertanov, L.; Nakatami, K. *J. Am. Chem. Soc.* **2000**, *122*, 9444. (b) Aldoshin, S. M.; Sanina, N. A.; Minkin, V. I.; Voloshin, N. A.; Ikorskii, V. N.; Ovcharenko, V. I.; Smirnov, V. A.; Nagaeva, N. K. *J. Mol. Struct.* **2007**, *826*, 69.
(7) Bénard, S.; Rivière, E.; Yu, P.; Nakatami, K.; Delouis, J. F. *Chem. Mater.* **2001**, *13*, 159.
(8) (a) Coronado, E.; Galán-Mascarós, J. R.; Gómez-García, C. J.; Laukhin, V. *Nature* **2000**, *408*, 447. (b) Alberola, A.; Coronado, E.; Galán-Mascarós, J. R.; Gimenez-Saiz, C.; Gómez-García, C. J. *J. Am. Chem. Soc.* **2003**, *125*, 10774. (c) Coronado, E.; Galán-Mascarós, J. R.; Gómez-García, C. J.; Martínez-Ferrero, E.; Van Smaalen, S. *Inorg. Chem.* **2004**, *43*, 4808.
(9) (a) Andrés, R.; Gruselle, M.; Malézieux, B.; Verdaguer, M.; Vaissermann, J. *Inorg. Chem.* **1999**, *38*, 4637. (b) Brissard, M.; Gruselle, M.; Malézieux, B.; Thouvenot, R.; Guyard-Duhayon, C.; Convert, O. *Eur. J. Inorg. Chem.* **2001**, 1745.
(10) Andrés, R.; Brissard, M.; Gruselle, M.; Train, C.; Vaissermann, J.; Malézieux, B.; Jamet, J. P.; Verdaguer, M. *Inorg. Chem.* **2001**, *40*, 4633.
(11) Clemente-León, M.; Coronado, E.; Dias, J. C.; Soriano-Portillo, A.; Willett, R. D. *Inorg. Chem.* **2008**, *47*, 6458.

10.1021/ic802341k CCC: $40.75 © 2009 American Chemical Society
Published on Web 03/02/2009

neighbors. The six oxygen atoms surrounding each transition-metal ion have the same relative positions in the 2D and 3D compounds. So discounting small changes due to the different locations of the cations, the local crystal-field environments experienced by the transition-metal ions in the 2D and 3D compounds would be identical. With almost the same separation between neighboring transition-metal ions bridged by an oxalate molecule, the nearest-neighbor exchange couplings in the 2D and 3D bimetallic oxalates should be approximately equal. Of course, materials with the same coordination number, local anisotropy, and exchange coupling are expected to exhibit similar magnetic behavior.

Yet the 2D and 3D bimetallic oxalates exhibit strikingly different magnetic properties. For example, the transition temperatures of the 3D materials are always lower than those of their 2D counterparts.[12,13] Whereas some 2D Fe(II)Fe(III) bimetallic oxalates exhibit magnetic compensation below T_c,[2] 3D Fe(II)Fe(III) bimetallic oxalates have shown no signs of magnetic compensation.[13,14] After re-examining the 3D structure, this paper uses a phenomenological model to show that most differences between these series of materials can be explained by the parallel alignment of the chiral anisotropy axis in the 2D compounds and their tetrahedral alignment in the 3D compounds.

Originally synthesized in 1992,[15] the 2D bimetallic oxalates $A[M(II)M'(III)(ox)_3]$ are layered molecule-based magnets with bimetallic layers separated by the organic cation A. Within each bimetallic layer, transition-metal ions M(II) and M′(III) are coupled by oxalate bridges on an open honeycomb lattice.[1] Depending on the metal atoms, the interactions within each bimetallic layer can be either ferromagnetic (FM) or antiferromagnetic (AF) (M(II) and M′(III) moments parallel or antiparallel) with moments pointing out of the plane. Each transition-metal ion M(II) or M′(III) is surrounded by six oxygen atoms that form two equilateral triangles, one a bit larger than the other and rotated by 48° with respect to each other. The chirality of the triangles around neighboring M(II) and M′(III) are opposite: if one set rotates clockwise (Δ), then the other set rotates counterclockwise (Λ). Transition temperatures as high as 45 K have been reported in the Fe(II)Fe(III) compounds.[2]

Soon after the 2D compounds were discovered, 3D bimetallic oxalates were synthesized by Decurtins et al.[16] In the 3D compounds, the chirality of the oxygen triangles around neighboring transition metals have the same sign (Δ − Δ or Λ − Λ), which forces the metal ions to fold into a 3D structure. Projected onto the *ab* plane, the 3D structure

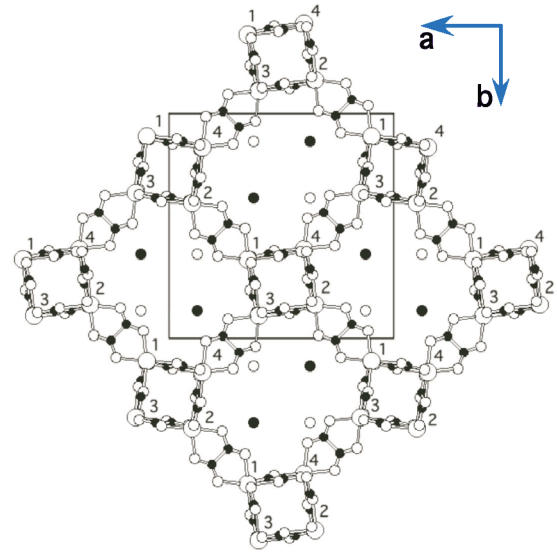

Figure 1. Projection of the 3D structure onto the *ab* plane, with a square denoting the unit cell. The chiral axis 1, 2, 3, or 4 (see Figure 2a) for each metal atom in the connected (10,3) anionic network is indicated. Inside the channels, metal atoms from the cations and water solvent molecules are drawn as filled and empty circles, respectively.

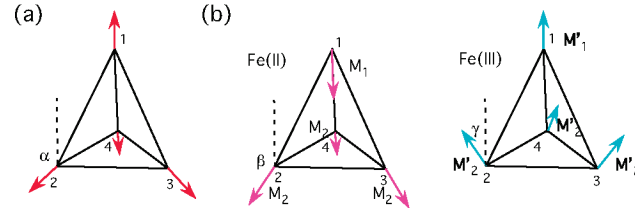

Figure 2. (a) Tetrahedral anisotropy axis $\mathbf{n}_k$ of a 3D bimetallic oxalate and (b) the order parameters M_k and M'_k and vectors $\mathbf{m}_k$ and $\mathbf{o}_k$ of the Fe(II) and Fe(III) spins of a 3D bimetallic oxalate. By symmetry, $M_2 = M_3 = M_4$ and $M'_2 = M'_3 = M'_4$.

is pictured in Figure 1. Each transition-metal ion connects back to itself through ten decagons that form a (10,3) anionic network.[17] Metal atoms from the cations and water solvent molecules are indicated by the filled and empty circles, respectively, inside the channels of Figure 1. Although the unit cell of the 3D compounds is cubic, the relative positions of the oxygen atoms around each transition-metal ion in the 2D and 3D compounds are approximately the same.[10,16]

The first 3D compounds were homometallic with every transition-metal ion M(II) coupled to three others through oxalate molecules.[16] Andrés et al.[10] and Coronado et al.[12,13] synthesized 3D bimetallic compounds by using the cations $[Z(II)(bpy)_3]^{2+}$ (Z = Ru, Fe, Co, or Ni) together with perchlorate ClO_4^- anions to maintain electroneutrality. Using cations with charge +1 rather than +2, Andrés et al.[10] and Clemente-León et al.[14] were able to synthesize 3D M(II)M′(III) bimetallic compounds without perchlorate anions. The sign of the exchange coupling between the transition metals M(II) and M′(III) in the 2D and 3D compounds remains the same, but the highest observed transition temperatures of the 3D compounds are always smaller than those of the 2D compounds.[14] In the Fe(II)Fe(III) bimetallic oxalates, T_c is about 40% smaller for the 3D compounds.

(12) Coronado, E.; Galán-Mascarós, J. R.; Gómez-García, C. J.; Martínez-Agudo, J. M. *Inorg. Chem.* **2001**, *40*, 113.
(13) Coronado, E.; Galán-Mascarós, J. R.; Gómez-García, C. J.; Martínez-Ferrero, E.; Almeida, M.; Waerenborgh, J. C. *Eur. J. Inorg. Chem.* **2005**, 2064.
(14) Clemente-León, M.; Coronado, E.; Gómez-García, C. J.; Soriano-Portillo, A. *Inorg. Chem.* **2006**, *45*, 5653.
(15) Tamaki, H.; Zhong, Z. J.; Matsumoto, N.; Kida, S.; Koikawa, M.; Achiwa, N.; Hashimoto, Y.; Ōkawa, H. *J. Am. Chem. Soc.* **1992**, *114*, 6974.
(16) (a) Decurtins, S.; Schmalle, H. W.; Schneuwly, P.; Oswald, H. R. *Inorg. Chem.* **1993**, *32*, 1888. (b) Decurtins, S.; Schmalle, H. W.; Schneuwly, P.; Ensling, J.; Gütlich, P. *J. Am. Chem. Soc.* **1994**, *116*, 9521.
(17) Decurtins, S.; Schmalle, H. W.; Pellaux, R.; Huber, R.; Fischer, P.; Ouladdiaf, B. *Adv. Mater.* **1996**, *8*, 647.

Because they are confined within small pockets, cations play a more important role in the 3D materials. In the 2D materials, the more rigid and compressible bimetallic planes can easily adjust to cations of different symmetries and sizes. Since the cations penetrate more deeply into the 3D bimetallic network, the transition temperature is more sensitive to the choice of cation[12−14] than in the 2D compounds.

For both the 2D and 3D compounds, the crystal-field potential V at the M(II) and M′(III) sites produced by the six nearby oxygen atoms has C_3 symmetry so that a rotation about the chiral axis by 120° leaves V unchanged. Earlier work[18,19] on the 2D compounds demonstrated that V splits the orbital-angular momentum L multiplet on each transition-metal ion into a set of orbital singlets and doublets. For example, the $L = 2$ multiplet on Fe(II) breaks into two doublets and one singlet but the $L' = 0$ singlet on Fe(III) is unaffected by the crystal-field potential. The average orbital angular momentum L_{cf} of a low-lying doublet can assume any real value between 0 and 2.

Because of the spin−orbit coupling $\lambda \mathbf{L}\cdot\mathbf{S}$, the magnetic moment on the Fe(II) sites may increase more rapidly with decreasing temperature than the Fe(III) moment. If the Fe(III) moment exceeds the Fe(II) moment at $T = 0$, this behavior produces magnetic compensation or a cancelation of the sublattice moments below T_c. In the 2D Fe(II)Fe(III) compounds, magnetic compensation was predicted[18] when L_{cf} is less than 1 but exceeds a lower threshold near 0.25. Whereas several papers[2] have documented the appearance of magnetic compensation in 2D Fe(II)Fe(III) compounds with certain cations, magnetic compensation has never been observed in a 3D Fe(II)Fe(III) compound.[13]

Upon re-examining the 3D structure, we conclude that most differences between the 2D and 3D materials can be explained by the tetrahedral coordination of the chiral axis in the 3D compounds. Our mean-field (MF) method is presented in Section II. Section III contains new results for the magnetization and transition temperature of the 3D Fe(II)Fe(III) bimetallic oxalates. Although results for the 2D Fe(II)Fe(III) compounds previously appeared in ref 18, they are summarized in Section III for comparison with our new 3D results. Section IV examines the 2D and 3D Mn(II)Cr(III) bimetallic oxalates, which are ferrromagnetic. The MF free energy of the 3D Fe(II)Fe(III) bimetallic oxalates is provided in the Appendix.

II. Chiral Structure and Methodology

While the local crystal-field environments in the 2D and 3D bimetallic oxalates are similar, the anisotropy axis in the 2D compounds all point in the **z** direction, perpendicular to the bimetallic planes. Consequently, the easy axis for the magnetization also points in the **z** direction, and the anisotropy at each site enhances the sublattice moment. Although some 2D Mn(II)Fe(III) bimetallic oxalates show signs of spin canting,[2b] almost all 2D compounds exhibit collinear magnetic order along the **z** axis.

An earlier analysis of the 3D crystal structure[12] erroneously concluded that the chiral or anisotropy axis of neighboring metal ions were perpendicular. A closer examination of the oxygen positions reveals that the chiral axis of any site and its three neighbors are tetrahedrally coordinated, as sketched in Figure 2a. In terms of the unit vectors, **a**, **b**, and **c** of the cubic 3D crystal structure, the tetrahedral directions are given by $\mathbf{n}_1 = (\mathbf{a} + \mathbf{b} + \mathbf{c})/\sqrt{3}$, $\mathbf{n}_2 = (-\mathbf{a} - \mathbf{b} + \mathbf{c})/\sqrt{3}$, $\mathbf{n}_3 = (\mathbf{a} - \mathbf{b} - \mathbf{c})/\sqrt{3}$, and $\mathbf{n}_4 = (-\mathbf{a} + \mathbf{b} - \mathbf{c})/\sqrt{3}$. Each chiral axis subtends an angle $\alpha = \cos^{-1}(-1/3) \approx 109.5°$ with any of the other three so that $\mathbf{n}_1 + \mathbf{n}_2 + \mathbf{n}_3 + \mathbf{n}_4 = 0$. The chiral axis for each metal ion of the projected 3D structure is indicated in Figure 1. As shown, the structural unit cell contains eight transition-metal ions: four M(II) ions and four M′(III) ions with chiral axis 1, 2, 3, or 4.

To model the 2D or 3D bimetallic oxalates, we assume that the energy separation between the lowest multiplet levels is much greater than the exchange coupling J and the spin−orbit coupling λ or λ' on that site. Both 2D and 3D bimetallic oxalates are then described by the Hamiltonian

$$H = -J\sum_{\langle ij\rangle} \mathbf{S}_i\cdot\mathbf{S}'_j + \lambda\sum_i \mathbf{L}_i\cdot\mathbf{S}_i + \lambda'\sum_j \mathbf{L}'_j\cdot\mathbf{S}'_j \qquad (1)$$

where the sums run over the M(II) sites i and the M′(III) sites j, and the exchange energy includes nearest neighbors only. The sign of the exchange constant J depends on whether the interactions between M(II) and M′(III) are ferromagnetic ($J > 0$) or antiferromagnetic ($J < 0$). On both the M(II) and M′(III) sites, we restrict consideration to the lowest-lying doublet or singlet in their orbital multiplets. Along the chiral axis **n** for those sites, $\mathbf{L}_i = \pm\mathbf{n}L_{cf}$ and $\mathbf{L}'_j = \pm\mathbf{n}L'_{cf}$ are the eigenvalues of the orbital angular momentum in the low-energy orbital doublets. When the singlet lies lowest in energy or an $L = 0$ ($L' = 0$) multiplet is not affected by the crystal field, then L_{cf} (L'_{cf}) would be taken to be zero. Of course, the chiral axis **n** for 2D compounds lies along the $\pm\mathbf{z}$ directions with opposite signs for the M(II) and M′(III) sublattices in each bimetallic layer.

We also assume that the magnetic moment **M** of a 3D bimetallic oxalate points along one of the four equivalent chiral directions $\mathbf{n}_k$. For simplicity, we take **M** to lie along $\mathbf{n}_1$. With the convention that $\mathbf{n}_1 = \mathbf{z}$, the four chiral axis are $\mathbf{n}_1 = (0,0,1)$, $\mathbf{n}_2 = (\sin\alpha, 0, \cos\alpha)$, $\mathbf{n}_3 = (-{}^1/_2 \sin\alpha, {}^{\sqrt{3}}/_2 \sin\alpha, \cos\alpha)$, and $\mathbf{n}_4 = (-{}^1/_2 \sin\alpha, -{}^{\sqrt{3}}/_2 \sin\alpha, \cos\alpha)$. All eight possible orientations $\pm\mathbf{n}_k$ for **M** will appear in different domains within the crystal. This is analogous to the case of a cubic ferromagnet, where the magnetization can point along the six directions $\pm\,\mathbf{a}$, $\pm\,\mathbf{b}$, and $\pm\,\mathbf{c}$.

Because of the non-collinear chiral axis, the magnetic moments on the M(II) and M′(III) sublattices will cant from the $\mathbf{n}_1$ direction. By symmetry, the magnitudes of the M(II) or M′(III) spins $M_k(T)$ or $M'_k(T)$ on sites with chiral axis $k = 2$, 3, or 4 are the same, but they can differ from the magnitudes of the M(II) or M′(III) spins $M_1(T)$ or $M'_1(T)$ on

(18) (a) Fishman, R. S.; Reboredo, F. A. *Phys. Rev. Lett.* **2007**, *99*, 217203. (b) Fishman, R. S.; Reboredo, F. A. *Phys. Rev. B* **2008**, *77*, 144421.
(19) Reis, P.; Fishman, R. S.; Reboredo, F. A.; Moreno, J. *Phys. Rev. B* **2008**, *77*, 174433.

sites with chiral axis 1. Therefore, the 3D bimetallic oxalates contain four rather than two spin order parameters. At $T = 0$, the M(II) or M′(III) spin expectation values all become equal with $M_k(T = 0) = S$ or $M'_k(T = 0) = S'$.

Quite generally, the internal field experienced by a transition-metal ion on a site with chiral axis 1 is the sum of the fields produced by ions on sites with chiral axis 2, 3, and 4. Since $\mathbf{n}_2 + \mathbf{n}_3 + \mathbf{n}_4 = -\mathbf{z}$, the net internal field must lie along the $\mathbf{z}$ direction. Similarly, the internal field experienced by a transition-metal ion on a site with chiral axis 2 is the sum of the fields produced by ions on sites with chiral axis 1, 3, and 4. Since spins on sites with chiral axis 1 have different magnitudes than spins on sites with chiral axis 3 or 4, and

$$\rho\mathbf{n}_1 + \mathbf{n}_3 + \mathbf{n}_4 = (\rho - 1)\mathbf{z} - \mathbf{n}_2 \qquad (2)$$

this net internal field has components along the $\mathbf{n}_2$ and $\mathbf{z}$ directions. It also follows that the net effective field at sites with chiral axis $\mathbf{n}_3$ or $\mathbf{n}_4$ has components along the $\mathbf{n}_3$ or $\mathbf{n}_4$ and $\mathbf{z}$ directions.

So for an antiferromagnetically coupled 3D bimetallic oxalate, the spins on the M(II) sublattice lie in the $\mathbf{m}_1 = -\mathbf{z}$ direction for sites with chiral axis 1 and in the $\mathbf{m}_2 = (\sin\beta, 0, \cos\beta)$, $\mathbf{m}_3 = (-{}^1/_2 \sin\beta, {}^{\sqrt{3}}/_2 \sin\beta, \cos\beta)$, or $\mathbf{m}4 = (-{}^1/_2 \sin\beta, -{}^{\sqrt{3}}/_2 \sin\beta, \cos\beta)$ directions for sites with chiral axis 2, 3, or 4. The spins on the M′(III) sublattice lie along the $\mathbf{o}_1 = \mathbf{n}_1$, $\mathbf{o}_2 = (\sin\gamma, 0, \cos\gamma)$, $\mathbf{o}_3 = (-{}^1/_2 \sin\gamma, {}^{\sqrt{3}}/_2 \sin\gamma, \cos\gamma)$, or $\mathbf{o}_4 = (-{}^1/_2 \sin\gamma, -{}^{\sqrt{3}}/_2 \sin\gamma, \cos\gamma)$ directions in the same fashion. As required from the general considerations above, $\mathbf{m}_k$ or $\mathbf{o}_k$ ($k = 2$, 3, or 4) has components along the $\mathbf{n}_k$ and $\mathbf{z}$ directions. Demanding that the effective internal field on a M′(III) site is parallel to the spin on that site fixes γ in terms of β. The remaining angle β must be determined by minimizing the free energy. Therefore, both β and γ depend on temperature.

Of course, the magnetization contains both spin and orbital contributions. While the spin may cant away from the chiral $\mathbf{n}_k$ direction, the orbital angular momentum always points along $\mathbf{n}_k$. The same symmetry arguments given above imply that the magnitudes of the orbital angular momenta $L_k(T)$ or $L'_k(T)$ on sites with chiral axis $k = 2$, 3, or 4 are the same but may differ from the magnitude of the orbital angular moments $L_1(T)$ or $L'_1(T)$ on sites with chiral axis 1. The orbital angular momenta are only identical at $T = 0$ with $L_k(T = 0) = L_{cf}$ and $L'_k(T = 0) = L'_{cf}$.

Therefore, symmetry considerations imply that the magnetic and structural unit cells of a 3D bimetallic oxalate are identical. Both contain four M(II) and four M′(III) ions, with chiral axis $k = 1$, 2, 3, and 4 and order parameters $M_1(T)$ or $M'_1(T)$ ($k = 1$) and $M_2(T)$ or $M'_2(T)$ ($k = 2$, 3, or 4).

Within MF theory, the Hamiltonian is given by

$$H_{MF} = -J\sum_{\langle ij\rangle}\{\mathbf{S}_i\cdot\langle\mathbf{S}'_j\rangle + \langle\mathbf{S}_i\rangle\cdot\mathbf{S}'_j - \langle\mathbf{S}_i\rangle\cdot\langle\mathbf{S}'_j\rangle\} + \lambda\sum_i \mathbf{L}_i\cdot\mathbf{S}_i + \lambda'\sum_j \mathbf{L}'_j\cdot\mathbf{S}'_j \qquad (3)$$

where the last term in the sum over nearest neighbors is included so as to count each interaction $-J\mathbf{S}_i\cdot\mathbf{S}'_j$ only once. Notice that the spin−orbit coupling is treated exactly and that only the exchange coupling is approximated within MF theory. Although eq 3 contains five degrees of freedom (four magnetic order parameters and the canting angle $\beta(T)$), its solution is straightforward.

To clarify this discussion, we specialize to the case of a 3D Fe(II)Fe(III) bimetallic oxalate, with spin−orbit coupling on the Fe(II) sites only. The order parameters $M_1(T)$ and $M_2(T)$ indicated in Figure 2b are the magnitudes of the Fe(II) spins on sites with chiral axis 1 and 2. Remember that sites with chiral axis 2, 3, and 4 all have the same magnitude for the spin and orbital moments. The order parameters $M'_1(T)$ and $M'_2(T)$ are the magnitudes of the Fe(III) spins on sites with chiral axis 1 and 2, 3, or 4. Since the orbital angular momentum is coupled ferromagnetically to the spin ($\lambda < 0$), the orbital moment on a site with chiral axis 1 is $-\mu_B L_2(T)\mathbf{z}$, and the total orbital moment of sites with chiral axis 2, 3, and 4 is $\mu_B L_2(T)(\mathbf{n}_2 + \mathbf{n}_3 + \mathbf{n}_4) = -\mu_B L_2(T)\mathbf{z}$. So the magnetic moment per pair of Fe(II) and Fe(III) spins is

$$\mathbf{M}(T) = \left\{\frac{3}{2}M_2\cos\beta - \frac{1}{2}M_1 - \frac{1}{4}(L_1 + L_2) + \frac{3}{2}M'_2\cos\gamma + \frac{1}{2}M'_1\right\}\mu_B\mathbf{z} \qquad (4)$$

All of the spin order parameters $M_k(T)$ and $M'_k(T)$, as well as the orbital momenta $L_k(T)$, are positive.

On the basis of eq 3, the effective internal field $\mathbf{h}_j$ experienced by an Fe(III) spin at site j is $\mathbf{h}_j = -J\sum'_i\langle\mathbf{S}_i\rangle$, where the primed sum runs over all nearest neighbors i of site j. Requiring that $\mathbf{h}_j$ is parallel to $\langle\mathbf{S}'_j\rangle$ provides the relation

$$\tan\gamma = \frac{M_2\sin\beta}{M_1 - 2M_2\cos\beta} \qquad (5)$$

So when all the Fe(II) spins point in the $-\mathbf{z}$ direction with $\beta = \pi$, all the Fe(III) spins would point in the $+\mathbf{z}$ direction with $\gamma = 0$. The canting angle $\beta(T)$ and the order parameters $M_1(T)$, $M_2(T)$, $M'_1(T)$, and $M'_2(T)$ are determined by minimizing the MF free energy $F_{MF}(M_k, M'_k, \beta)$ given in the Appendix.

The formalism for ferromagnetically coupled 3D bimetallic oxalates like the Mn(II)Cr(III) system is a straightforward generalization. The only important difference is that now both the M(II) and the M′(III) spins on sites with chiral axis 1 point in the $+\mathbf{z}$ direction. Detailed results for the ferrimagnet Fe(II)Fe(III) and the ferromagnet Mn(II)Cr(III) are presented in the next two sections.

III. Fe(II)Fe(III) Bimetallic Oxalates

Spin−orbit coupling in the Fe(II)Fe(III) bimetallic oxalates is present on the $S = 2$ Fe(II) sites only with $\lambda \approx -12.5$ meV, so the orbital and spin moments are coupled ferromagnetically. There is no spin−orbit coupling on the $S' = 5/2$ Fe(III) sites. The four magnetic order parameters and the canting angle β are obtained by minimizing the MF free energy F_{MF} given in the Appendix. The magnetizations $M(T)$ of the 2D and 3D Fe(II)Fe(III) bimetallic oxalates per pair of Fe(II) and Fe(III) sites are plotted in Figure 3, both with

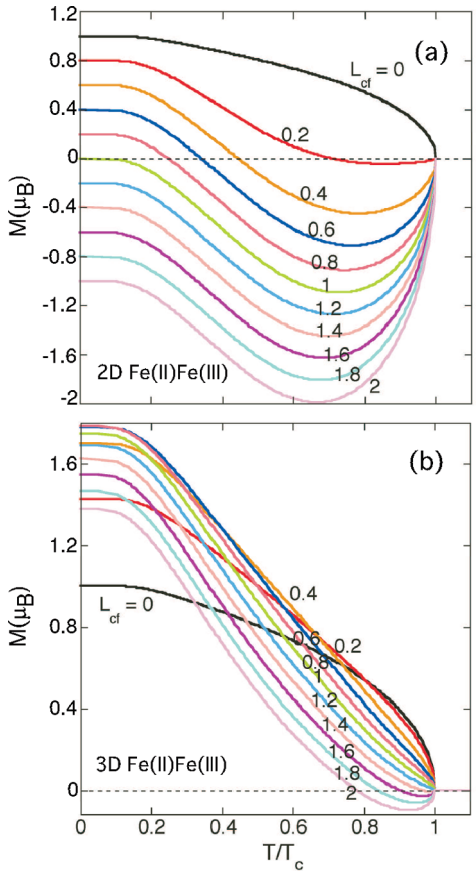

Figure 3. Temperature-dependence of the magnetization for the (a) 2D and (b) 3D Fe(II)Fe(III) bimetallic oxalates with $|\lambda/J| = 37.5$ and several values of L_{cf}.

$|\lambda/J| = 37.5$. Whereas the Fe(III) moments with $\cos\gamma > 0$ contribute positively to M, the Fe(II) moments with $\cos\beta < 0$ contribute negatively. For the 2D magnetization plotted in Figure 3a, magnetic compensation appears in the window $0.18 < L_{cf} < 1$. When $L_{cf} \geq 1$, the Fe(II) moment dominates for all temperatures and $M < 0$. By contrast, Figure 3b indicates that in 3D compounds, the Fe(III) moment is always larger than the Fe(II) moment at $T = 0$. Magnetic compensation is found only for $2 \geq L_{cf} > 1.29$ and even then, the negative magnetization is rather shallow with T_{comp} quite close to T_c.

The threshold value for compensation in the 3D compounds is plotted in Figure 4, where the curve separates a region with no compensation points $n_{comp} = 0$ from a region with $n_{comp} = 1$. We find that the threshold value for L_{cf} is a non-monotonic function of $|\lambda/J|$ with a minimum of about 1.24 at $|\lambda/J| \approx 20$. For smaller values of $|\lambda/J|$, the threshold rises quite rapidly. There is no indication of the $n_{comp} = 2$ region that appeared in the phase diagram of the 2D compounds.[18] On the basis of that earlier study of 2D compounds, the large values of L_{cf} required for compensation in the 3D compounds would seem rather unlikely.

Notice that the 3D magnetization in Figure 3b is a non-monotonic function of L_{cf} at $T = 0$. For $L_{cf} = 0$, all the Fe(II) spins point in the $-\mathbf{z}$ direction while all the Fe(III) spins point in the $+\mathbf{z}$ direction so that $M(T = 0) = 1\ \mu_B$. As L_{cf} increases, the Fe(II) spins cant upward, the Fe(III) spins cant downward, and the orbital contribution to the net moment

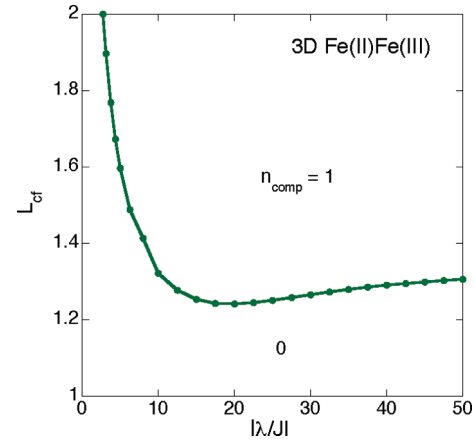

Figure 4. Threshold value of L_{cf} for 3D Fe(II)Fe(III) bimetallic oxalates versus $|\lambda/J|$.

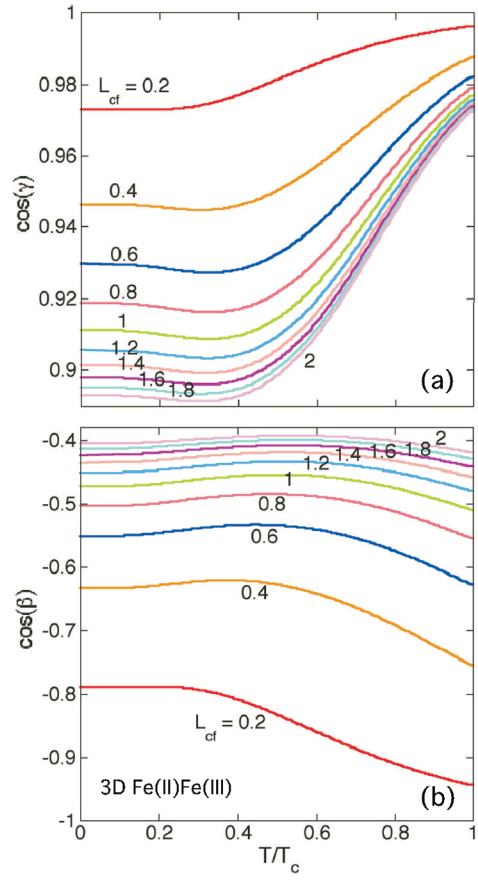

Figure 5. Temperature dependence of the canting angles β (Fe(II)) and γ (Fe(III)) in 3D Fe(II)Fe(III) bimetallic oxalates using the same parameters as in Figure 3.

reduces $M(0)$. Because of these competing effects, $M(T = 0)$ reaches a maximum of about 1.78 μ_B at $L_{cf} \approx 0.7$.

In Figure 5, we plot the temperature dependence of the canting angles $\beta(T)$ and $\gamma(T)$ for the Fe(III) and Fe(II) spins, respectively, on sites with chiral axis 2, 3, or 4. Because the spin−orbit coupling is absent on the Fe(III) sites, the canting of the Fe(III) spins is much more modest than the canting of the Fe(II) spins. With $L_{cf} = 2$, the canting angle $\beta(T)$ plotted in Figure 5a is only about 27° at low temperatures, decreasing to about 14° at T_c. By contrast, the canting angle $\beta(T)$ plotted in Figure 5b remains close to 114° for all

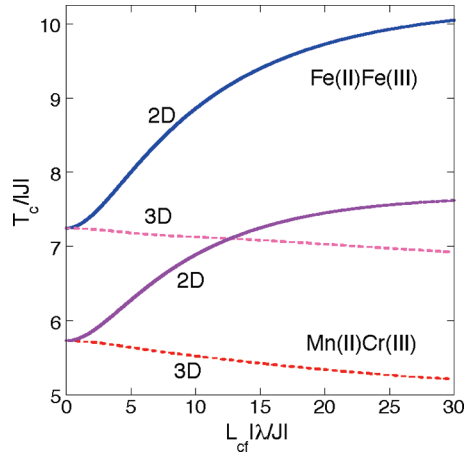

Figure 6. Transition temperatures of the 2D (solid) and 3D (dashed) Fe(II)Fe(III) and Mn(II)Cr(III) bimetallic oxalates versus $L_{cf}|\lambda/J|$.

temperatures. Of course, $\beta(T)\rightarrow\alpha \approx 109.5°$ and $\cos\beta(T)\rightarrow -1/3$ as $|\lambda/J|\rightarrow\infty$.

The transition temperatures of both 2D and 3D Fe(II)Fe(III) bimetallic oxalates are plotted in the upper curves of Figure 6. Because T_c does not directly involve the orbital contribution to the magnetization, it only depends on J and the product λL_{cf}. When $L_{cf} = 0$, $T_c = [S(S+1)S'(S'+1)]^{1/2}|J| \approx 7.25|J|$ for both the 2D and 3D compounds. As L_{cf} increases, the 2D transition temperature rises, but the 3D transition temperature falls. They approach the limits $10.25J$ and $6.56J$ as $L_{cf}|\lambda/J|\rightarrow\infty$. The suppression of T_c with L_{cf} in the 3D compounds is caused by the magnetic frustration associated with the non-parallel chiral axis: because of the tetrahedral coordination of the chiral axis, an Fe(II) moment cannot minimize the antiferromagnetic exchange energy with each of its Fe(III) neighbors. Experimentally, the highest 3D transition temperature of 28 K[14] is about 40% lower than the highest 2D transition temperature of 45 K.[2]

However, by decoupling magnetic fluctuations on neighboring sites, MF theory always overestimates T_c. Even more seriously, MF theory yields a nonzero transition temperature in the limit $L_{cf}\rightarrow 0$. For 2D systems with short-ranged interactions, the Mermin−Wagner theorem[20] states that gapless spin fluctuations will destroy long-range magnetic order at nonzero temperatures. Hence, the transition temperature of 2D compounds must vanish in the absence of spin−orbit anisotropy. A recent Monte-Carlo analysis[21] of the 2D Fe(II)Fe(III) bimetallic oxalates confirms that $T_c\rightarrow 0$ as $L_{cf}\rightarrow 0$ and that MF theory overestimates $T_c/|J|$ by about 40% for $L_{cf}|\lambda/J| \gg 1$. Nevertheless, Monte-Carlo simulations qualitatively confirmed the most important predictions of MF theory: the appearance of magnetic compensation for L_{cf} above a threshold close to 0.25 and below 1, and the increase of the transition temperature with L_{cf}.

The transition temperature of 3D compounds does not vanish as $L_{cf}\rightarrow 0$ because the Mermin−Wagner theorem[20] applies only to topologically 2D systems. But for large $L_{cf}|\lambda/J|$, Figure 6 still indicates that $T_c/|J|$ is expected to be about 35% smaller for the 3D than for the 2D Fe(II)Fe(III) compounds. Using the values, $L_{cf} \approx 0.35$, $J \approx 0.45$ meV, and $L_{cf}|\lambda/J| \approx 9.7$ believed to describe the 2D Fe(II)Fe(III) compounds,[18] T_c should be about 20% smaller for 3D compounds. This accounts for roughly half of the observed suppression of T_c in the 3D compounds. The remaining 20% suppression of T_c may be partly caused by two effects that reduce the 3D exchange parameter: the smaller orbital overlap because of the distortion of the oxalate bridges[10] and the slightly larger metal-to-metal distances.[12,13] In addition, the anisotropy may be lower in 3D compounds because of the proximity of the organic cations, which can break the C_3 symmetry of the crystal-field potential[22] about each Fe(II) ion. The closer proximity of the cations in the 3D compounds may also suppress T_c by introducing structural disorder into the anionic network.

IV. Mn(II)Cr(III) Bimetallic Oxalates

We have also used MF theory to investigate the ferromagnetic Mn(II)Cr(III) compounds. Since the $S = 5/2$ Mn(II) $3d^5$ multiplets are orbital singlets, the $S' = 3/2$ Cr(III) $3d^3$ multiplets must be responsible for any magnetic anisotropy. Because of the positive spin−orbit coupling constant on the Cr(III) sites $\lambda \approx 11.3$ meV (called λ rather than λ' to facilitate comparison with the Fe(II)Fe(III) results), the orbital angular momentum $\mathbf{L}'_j$ is antiferromagnetically coupled to the Cr(III) spins $\mathbf{S}'_j$.

If the orbital-correlation energy within the Cr(III) $3d^3$ multiplet were weak, then Hund's second law would not be obeyed and the total orbital angular momentum would not be a good quantum number. Consequently, the $L' = 2$ multiplet of uncorrelated levels would be split by the crystal-field potential into two doublets and one singlet, as for Fe(II). Since these independent levels would be filled sequentially by the three electrons, a nonzero average orbital angular momentum L_{cf} would require that the singlet lies above the two doublets in energy. For any other configuration, L_{cf} would vanish. On the other hand, if the orbital-correlation energy were strong, then the total orbital angular momentum would be a good quantum number with $L' = 3$. The crystal-field potential would split this 7-fold degenerate level into three doublets and one singlet. A nonzero L_{cf} would then require that one of the three doublets lies lowest in energy. This latter scenario may be more likely than the first.

Nonzero anisotropy reduces the moment M in two ways. First, on sites with chiral axis 2, 3, or 4, the spin−orbit coupling cants the Mn(II) and Cr(III) spins away from the $\mathbf{z}$ direction. Second, the total moment is reduced by the orbital contribution in the $-\mathbf{z}$ direction. Consequently, the $T = 0$ magnetization decreases monotonically with increasing L_{cf}.

In Figure 6, we plot the transition temperatures of 2D and 3D Mn(II)Cr(III) bimetallic oxalates versus $L_{cf}|\lambda/J|$. At $L_{cf} = 0$, $T_c = [S(S+1)S'(S'+1)]^{1/2}|J| \approx 5.73|J|$ for both 2D and 3D compounds. Experimentally, the transition temper-

(20) Mermin, N.; Wagner, H. *Phys. Rev. Lett.* **1964**, *17*, 1133.
(21) Henelius, P.; Fishman, R. S. *Phys. Rev. B* **2008**, *78*, 214405.
(22) (a) Fishman, R. S.; Okamoto, S.; Reboredo, F. A. *Phys. Rev. Lett.* **2008**, *101*, 116402. (b) Fishman, R. S.; Okamoto, S.; Reboredo, F. A. *Polyhedron* DOI: 10.1016/j.poly 2008.11.007.

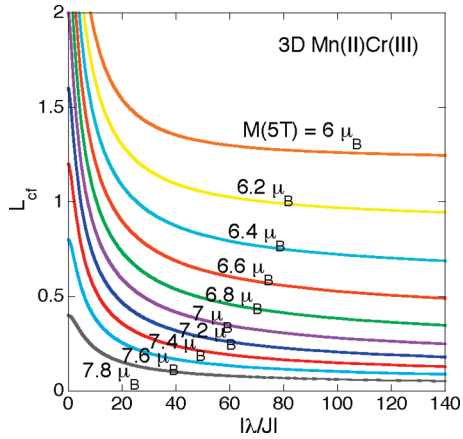

Figure 7. L_{cf} values for 3D Mn(II)Cr(III) compounds that are compatible with the observed low-temperature magnetization in a 5 T field.

ature $T_c \approx 5$ K of 3D Mn(II)Cr(III) compounds is reduced by about 15% from its 2D value of 6 K.[14]

For a Mn(II)Cr(III) ferromagnet without anisotropy, the $T = 0$ moment is $M = 2\,\mu_B(S + S') = 8\,\mu_B$. Because of the parallel anisotropy axis, the magnetization of a 2D compound reaches its saturation value $M^{sat} = 2\,\mu_B(S + S' - L_{cf}/2)$ very rapidly in applied field. In a 2D Mn(II)Cr(III) compound, the observed saturation moment[15] M^{sat} above 5 T is 7.74 μ_B, corresponding to $L_{cf} = 0.26$ for the orbital anisotropy. Our MF result for T_c then produces the 2D exchange parameter $|J| \approx 0.068$ meV.

As expected for a canted ferromagnet, the moment $M(H)$ of the 3D compounds increases rather slowly with applied magnetic field H. Since the orbital moments cannot rotate away from the chiral axis $\mathbf{n}_k$, the expected saturation moment in very large fields is $M^{sat} = 2\mu_B(S + S' - L_{cf}/4)$. But even at 5 T, M(5 T) does not appear to have reached its saturation limit and varies from 6.7 to 7.5 μ_B, depending on the cation.[12,23,24]

To interpret these measurements, we have evaluated the $T = 0$ magnetic moment $M(H)$ of 3D compounds at $H = 5$ T. For a given value of M(5 T) the required value of L_{cf} is plotted versus $|\lambda/J|$ in Figure 7. Of course, smaller values of M(5 T) require larger values of L_{cf}. The required value of L_{cf} decreases with increasing $|\lambda/J|$. For $|\lambda/J| \approx 140$ (see below), Figure 7 suggests that L_{cf} must lie between about 0.1 (M(5 T) = 7.5 μ_B, M^{sat} = 7.95 μ_B) and 0.4 (M(5 T) = 6.7 μ_B, M^{sat} = 7.8 μ_B). On the other hand, the measured moment[25] of 7.8 μ_B in a field of 9 T corresponds to a smaller anisotropy of $L_{cf} \approx 0.07$.

By contrast, recent neutron-scattering measurements[23] on a 3D Mn(II)Cr(III) powder find no signature of canting and yield magnetic moments that are only slightly below their spin-only values. For example, the observed Cr(III) moment of 2.9 μ_B is only slightly less than the expected spin-only value of 3 μ_B. The total zero-field moment $M(0) \approx 7.5\,\mu_B$ corresponds to an anisotropy of $L_{cf} \approx 0.04$, below the smallest estimate obtained from the magnetization measurements at 5 or 9 T.

Fitting the 3D transition temperature of 5 K using $L_{cf} \leq 0.1$ yields an exchange parameter $|J| \approx 0.078$ meV, which is somewhat larger than the 2D estimate of 0.068 meV. An anisotropy of $L_{cf} \approx 0.4$ corresponds to only slightly larger values of $|J| \approx 0.083$ meV. These estimates imply that $|\lambda/J| \approx 140$, the ratio used above in our estimate for L_{cf} from the magnetization measurements.

So the magnetization and neutron-scattering measurements on the 3D compounds disagree. Whereas magnetization measurements provide evidence for spin canting with an orbital anisotropy $L_{cf} \geq 0.07$, neutron-scattering measurements suggest that the anisotropy $L_{cf} \approx 0.04$ is much weaker. With an anisotropy of $L_{cf} \approx 0.04$, the zero-field moment $M(0) \approx 7.5\,\mu_B$ observed using neutrons should increase to about M(5 T) $\approx$ 7.85 μ_B at 5 T, larger than found in any magnetization measurement. Supporting the neutron-scattering results, however, coercivity measurements[10] on Ni(II)-Cr(III) bimetallic oxalates also suggest that the anisotropy is much weaker in 3D than in 2D compounds.

V. Conclusion

As already conjectured,[12] the differences between the magnetic properties of the 2D and 3D series of bimetallic oxalates can be explained by the non-collinear alignment of the chiral axis in the 3D compounds. Although the local crystal-field environment is unchanged by the non-collinearity of the anisotropy axis, the 3D transition temperatures of the Fe(II)Fe(III) compounds are reduced by about 20% compared with the 2D result. The condition for magnetic compensation in the 3D Fe(II)Fe(III) compounds is also much more difficult to achieve than in the 2D compounds. It seems highly unlikely that the large values for L_{cf} required for compensation in the 3D compounds can be reached.

Indeed, the closer proximity of the cations to the transition-metal ions in the 3D compounds will act to break the local C_3 symmetry and to reduce L_{cf} compared to its 2D value.[22] This effect may be responsible for the lower anisotropy found in the 3D Mn(II)Cr(III) compounds by coercivity[10] and neutron-scattering[23] measurements. It may also cause the sensitivity of T_c to the choice of cation in the 3D compounds.[12,13]

Associated with the four chiral axis and two orientations, eight magnetic domains will appear in any 3D sample. Applying strain in one of the four chiral directions will favor two domains over the other six. So strain may produce a dramatic increase in the spontaneous magnetic moment of a 3D ferromagnetic Mn(II)Cr(III) compound.

By using an Fe(II) spin-crossover templating cation, Coronado et al.[26] were very recently able to synthesize achiral 3D Mn(II)Cr(III) bimetallic oxalates, with alternating Δ and Λ chiralities on the Mn(II) and Cr(III) sites. The achiral 3D compounds have some important differences with

(23) Pontillart, F.; Gruselle, M.; André, G.; Train, C. *J. Phys.: Cond. Mat.* **2008**, *20*, 135214.
(24) We discount the small value $M(5T) = 6\,\mu_B$ obtained in a compound with an Fe-based cation.[12] The low value of $M(5T)$ may be caused by the substitution of $S' = 5/2$ Fe(III) ions into the Fe(II) sublattice.
(25) Clemente-León, M. (unpublished).
(26) Coronado, E.; Galán-Mascarós, J. R.; Giménez-López, M. C.; Almeida, M.; Waerenborgh, J. C. *Polyhedron* **2007**, *26*, 1838.

the chiral 3D compounds discussed in this paper. In particular, the unit cell is no longer cubic, and the coordination of the chiral anisotropy axis is no longer tetrahedral. We may examine the achiral compounds more closely in future work.

This paper once again underscores the close connection between the structural and magnetic properties of molecule-based magnets. Although the crystal-field environment of the transition-metal ions in the 2D and 3D series of bimetallic oxalates are similar, the tetrahedral coordination of the chiral axis in the 3D compounds has profound consequences for the magnetic properties of those materials. Hopefully, future neutron-scattering measurements on large 3D single crystals will confirm our results. We also hope that this paper will inspire future investigations of molecule-based magnets using phenomenological models based on symmetry and energy considerations.

Acknowledgment. We would like to acknowledge conversations with Drs. Satoshi Okamoto and Fernando Reboredo. This research was sponsored by the Division of Materials Science and Engineering of the U.S. Department of Energy and by the Spanish Ministerio de Ciencia e Innovacion (Project Consolider-Ingenio in Molecular Nanoscience CSD2007-00010, and projects CTQ2005-09385-C03 and MAT2007-61584).

MF Free Energy

The MF free energy for the 3D Fe(II)Fe(III) bimetallic oxalates is

$$\frac{F_{\mathrm{MF}}}{N} = -T\log\{Z_1 Z_1'(Z_2 Z_2')^3\} + 3|J|\{\cos\gamma\, M_1 M_1' - (2\cos\beta\cos\gamma - \sin\beta\sin\gamma)M_2 M_2' - \cos\beta\, M_2 M_1'\} \quad \text{(A1)}$$

where N is the number of magnetic or structural unit cells, each containing four Fe(II) sites and four Fe(III) sites. The terms to the right of the partition functions correspond to the last term in the brackets of the MF Hamiltonian of eq 3, which was introduced to avoid overcounting. The Fe(III) canting angle γ is given in terms of the Fe(II) canting angle β by eq 5. Recall that $\cos\alpha = -1/3$ and $\sin\alpha = 2\sqrt{2}/3$ for the tetrahedral angle α.

The Fe(II) or Fe(III) partition function on the magnetic sublattice with chiral axis 1 is Z_1 or Z'_1. By symmetry, the Fe(II) or Fe(III) sublattices with chiral axis 2, 3, and 4 all share the same partition function Z_2 or Z'_2. The MF partition functions Z_1 and Z_2 on the Fe(II) sites are

$$Z_1 = 2\sum_{\sigma} e^{3|J|M_2'\cos\gamma\,\sigma/T}\cosh(|\lambda|L_{\mathrm{cf}}\sigma/T) \quad \text{(A2)}$$

$$Z_2 = \sum_{\sigma}(e^{-\epsilon_\sigma^{(1)}/T} + e^{-\epsilon_\sigma^{(2)}/T}) \quad \text{(A3)}$$

where the σ sum runs from -2 to 2 and

$$\epsilon_\sigma^{(1)} = -|J|\sigma\{(M_2'\sin\gamma + L_{\mathrm{cf}}|\lambda/J|\sin\alpha)^2 + (M_1' + 2M_2'\cos\gamma - L_{\mathrm{cf}}|\lambda/J|\cos\alpha)^2\}^{1/2} \quad \text{(A4)}$$

$$\epsilon_\sigma^{(2)} = -|J|\sigma\{(M_2'\sin\gamma - L_{\mathrm{cf}}|\lambda/J|\sin\alpha)^2 + (M_1' + 2M_2'\cos\gamma + L_{\mathrm{cf}}|\lambda/J|\cos\alpha)^2\}^{1/2} \quad \text{(A5)}$$

are the MF eigenvalues on Fe(II) sites with chiral axis 2, 3, or 4. The MF partition functions Z'_1 and Z'_2 on the Fe(III) sites are

$$Z_1' = \sum_{\sigma'} e^{-3|J|M_2\cos\beta\,\sigma'/T} \quad \text{(A6)}$$

$$Z_2' = \sum_{\sigma'}\exp\{|J|\sigma'(M_1\cos\gamma - M_2(2\cos\gamma\cos\beta - \sin\gamma\sin\beta))/T\} \quad \text{(A7)}$$

where the σ' sum runs from $-5/2$ to $+5/2$.

IC802341K